Bounds on the Z' mass and mixing angles in the ununified gauge models

Debasis Bhowmick, Krishnanath Bandyopadhyay, and Asim K. Ray
Department of Physics, Visva-Bharati University, Santiniketan 731 235, West Bengal, India

Utpal Sarkar
Theory Group, Physical Research Laboratory, Ahmedabad 380009, India
(Received 7 April 1994)

We calculate the total cross sections and forward-backward asymmetries in $e^+e^- \to f\bar{f}$ processes with all possible leptonic and hadronic channels in the ununified models for a wide range of center-of-mass energy and then compare our results with those calculated in the standard model, taking into consideration the $Z - Z'$ mixing in the ununified models. We show that both ununified models cannot be distinguished from the standard model through the measurment of the above parameters. Interestingly, the mixing angles of these ununified models are severely constrained from the measured CERN LEP data, which ultimately leads to a Z' mass of more than 1 TeV.

PACS number(s): 13.65.+i, 12.10.Dm, 12.60.Cn, 14.70.Pw

I. INTRODUCTION

The precision measurements at the CERN e^+e^- collider LEP [1] has stimulated the search for the nonstandard signature of Z', the extra Z boson originating in the extensions of the standard model (SM) [2], such as the left-right-symmetric (LRS) model [3] and the gauge models [η, χ, ψ , alternate LRS (ALRS)] emerging at low energies from the superstring-inspired E_6 model [4]. In the presence of one extra Z, there are two mass eigenstates Z_L and Z_H with masses M_{Z_L} and M_{Z_H} ($M_{Z_L} \ll M_{Z_H}$), which are related to the weak eigenstates Z_1 and Z_2 by a mixing angle ϕ. The analysis [5] of the above models has established the bounds on the Z' mass, the mixing angle, and the contribution due to Z' to the ρ parameter of the SM. It would, therefore, be interesting to make a similar analysis for the ununified models [6, 7] which have extended gauge sectors with extra Z bosons.

The partially ununified model (PUM) [6] based on the gauge group $SU(2)_q \times SU(2)_l \times U(1)_Y$ ununifies partially in the sense that the left-handed quarks and leptons couple to different SU(2)-gauge groups and the right-handed fermions tranform as singlets under both. The other model [7] referred to as the fully ununified model (FUM) is based on the gauge group $G_{qL} \times G_{lL}$, where $G_{qL} = SU(2)_{qL} \times U(1)_{Y_q}$ and $G_{lL} = SU(2)_{lL} \times U(1)_{Y_l}$. The quarks (leptons) transform under G_{qL} (G_{lL}) exactly in the same way as they do under the SM and as a singlet under $G_{lL}(G_{qL})$. Although both the PUM and FUM have an identical number of charged gauge bosons, the PUM has one extra Z boson (Z_H) while the FUM has two extra Z bosons (Z_H and Z_S). In the context of the PUM some phenomenological studies have already been carried out [8] to constrain the model parameters using the precision LEP data on the leptonic and hadronic decay widths of the weak charged and neutral gauge bosons and forward-backward (FB) asymmetry in the $e^+e^- \to \mu^+\mu^-, b\bar{b}$ processes. Recently, we have calculated [9] the left-right and the charge asymmetry parameters [A, B, C_L, C_R] in the e-p and e-d deep-inelastic scattering processes at $Q^2 = 1$ GeV$^2/c^2$ within the framework of the ununified models and found that these models cannot be discriminated from the SM, except for the measurement of C_R, which again is not feasible at present. This has motivated us to look for the signature of the extra Z boson in the PUM and FUM using precision measurements at LEP.

In the present paper we have calculated the hadronic and leptonic cross sections and angular FB asymmetries in $e^+e^- \to l\bar{l}, q\bar{q}$ processes for the same set of model parameters [ratio of vacuum expectation values (VEV's) of Higgs scalars and mixing angle] used in Ref. [9] and compared these values with those in the SM. Furthermore, we have also determined the bounds on the masses of the extra Z bosons, their mixing angles and their contributions to the ρ parameter from a fit to the precision LEP data on $\Gamma_Z, \sigma^h_{\rm peak}, R = \frac{\Gamma_h}{\Gamma_l}, A^l_{\rm FB}(M_z^2), A^b_{\rm FB}(M_z^2), A^\tau_{\rm pol}(M_z^2)$.

Our study shows that the PUM as well as the FUM cannot be discriminated from the SM through the measurement of total cross section in the unit of point cross section and FB-asymmetry parameters with a c.m. energy $\sqrt{s}$ within the range 40 GeV $\leq \sqrt{s} \leq$ 160 GeV for $e^+e^- \to l\bar{l}, q\bar{q}$ processes. Moreover, a simultaneous fit of all the observables from both the leptonic and hadronic channels severely constrains the mixing angles and thereby leads to a lower bound of 1 TeV on the extra Z mass.

The organization of this paper is as follows. In Sec. II, we describe briefly the models. Section III contains a brief discussion on the radiative corrections and the formulas for the decay widths of Z, cross sections, and the FB asymmetries for the $e^+e^- \to f\bar{f}$ processes. Our results are presented in Sec. IV, and conclusions are given in Sec. V.

II. THE MODEL

We mention here briefly the essential features of the two ununified models. In the PUM the fermion couplings to the neutral gauge bosons in a convenient basis are given by

$$\frac{g}{C_W}\left(T_{3q}+T_{3l}-S_W^2 Q\right) Z_1{}^{\mu}+g\left(\frac{C_\phi}{S_\phi}T_{3q}-\frac{S_\phi}{C_\phi}T_{3l}\right) Z_2^{\mu}\ , \tag{1}$$

where g is the usual weak coupling constant, $T_{3l(q)}$ is the third component of weak isospin for $\mathrm{SU}(2)_{l(q)}$ group, Q is the electric charge, θ_W is the Weinberg angle, and ϕ is the new additional mixing angle, with $S_\phi=\sin\phi$, $C_\phi=\cos\phi$, $C_W=\cos\theta_W$, $S_W=\sin\theta_W$. The symmetry breaking occurs when two scalar fields $\Sigma(2,2,0)$ and $\phi(1,2,\frac{1}{2})$ acquire vacuum expectation values (VEV's):

$$\langle\phi\rangle=\begin{pmatrix}0\\ \frac{v}{\sqrt{2}}\end{pmatrix}\qquad \langle\Sigma\rangle=\begin{pmatrix}u&0\\0&u\end{pmatrix}. \tag{2}$$

The ratio $x=\frac{u^2}{v^2}$ and new mixing angle ϕ are two parameters of the model. By the conventional orthogonal transformation we diagonalize the $Z_1{}^{\mu}$-$Z_2{}^{\mu}$ mass matrix and assuming $S_\phi^2\ll 1$ the masses of the Z boson are given by

$$M_{Z_L}\sim M_Z\left(1-\frac{S_\phi^4}{2x}\right)\ ,$$
$$M_{Z_H}\sim\frac{M_W\sqrt{x}}{S_\phi C_\phi}\left(1+\frac{S_\phi^4}{2x}\right)\ . \tag{3}$$

In the approximation $\frac{x}{S_\phi^2}\gg 1$ the corresponding mass eigenstates are given by

$$Z_L\sim Z_1+\frac{S_\phi{}^3C_\phi}{xC_W}Z_2\ ,$$
$$Z_H\sim Z_2-\frac{S_\phi{}^3C_\phi}{xC_W}Z_1. \tag{4}$$

In a different parametrization, instead of taking x and ϕ as two arbitrary parameters we can replace

$$x\simeq S_\phi^2\left[C_\phi^2\left(1+\frac{m_{ZH}^2}{m_W^2}\right)-1\right] \tag{5}$$

and thereby we can treat ϕ and M_{Z_H} as two arbitrary parameters also. Similarly in the FUM the corresponding fermion coupling to the neutral gauge bosons are

$$g t_W\left(t_\theta^{-1}Y_q-t_\theta Y_l\right) Z_1^{\mu}+g\left(t_\phi^{-1}T_q^3-t_\phi T_l^3\right) Z_n^{\mu}$$
$$+gC_W^{-1}\left(T_d^3-S_W^2 Q\right) Z_d^{\mu}. \tag{6}$$

Here $T_d^i=T_q^i+T_l^i$ with $C_i=\cos\theta_i$; $S_i=\sin\theta_i$; $t_i=\tan\theta_i$; $i=w,\phi,\theta$; ϕ and θ are the additional mixing angles in this model. The minimal Higgs fields chosen in the model are $\phi_q(2,\frac{1}{2},1,0)$, $\phi_l(1,0,2,\frac{1}{2})$, $\Sigma(1,\frac{1}{6},1,-\frac{1}{6})$, and $H(2,0,2,0)$. H is the real field and is responsible for the breaking of $\mathrm{SU}(2)_{qL}\times\mathrm{SU}(2)_{lL}$ to diagonal $\mathrm{SU}(2)_L$. The nonzero VEV of Σ breaks $U(1)_{Y_q}\times U(1)_{Y_l}$ to $U(1)_Y$. ϕ_q and ϕ_l are used to break the standard electroweak symmetry giving masses to quarks and leptons, respectively.

The choice of the VEV's of the Higgs fields are

$$\langle H\rangle=\begin{pmatrix}u&0\\0&u\end{pmatrix},\quad \langle\Sigma\rangle=\sigma\ ,$$
$$\langle\phi_q\rangle=\begin{pmatrix}0\\ v_q\end{pmatrix},\quad \langle\phi_l\rangle=(0\cdot v_l). \tag{7}$$

The mass eigenstates of the neutral gauge bosons are

$$\begin{pmatrix}Z_S\\Z_H\\Z_L\end{pmatrix}=\begin{pmatrix}1&0&0\\0&C_{nd}&-S_{nd}\\0&S_{nd}&C_{nd}\end{pmatrix}\begin{pmatrix}C_{ld}&0&-S_{ld}\\0&1&0\\S_{ld}&0&C_{ld}\end{pmatrix}$$
$$\times\begin{pmatrix}C_{nl}&-S_{nl}&0\\S_{nl}&C_{nl}&0\\0&0&1\end{pmatrix}\begin{pmatrix}Z_l\\Z_n\\Z_d\end{pmatrix}\ , \tag{8}$$

where

$$\tan\theta_{nd}\sim\frac{q_nq_d-l_nl_d}{m_n^2+l_n^2+q_n^2-l_d^2-q_d^2},$$
$$\tan\theta_{ld}\sim\frac{l_ll_d-q_lq_d}{m_l^2+l_l^2+q_l^2-l_d^2-q_d^2},$$
$$\tan\theta_{nl}\sim\frac{q_lq_n+l_ll_n}{m_l^2+l_l^2+q_l^2-m_n^2-l_n^2-q_n^2}, \tag{9}$$

$$m_l{}^2=\frac{4a^2\sigma^2}{C_\theta{}^2S_\theta{}^2},\quad m_n{}^2=\frac{2u^2}{C_\phi{}^2S_\phi{}^2},$$
$$l_l=v_lt_Wt_\theta,\quad l_n=v_qt_\phi,$$
$$l_d=v_lC_W{}^{-1},\quad q_l=v_qt_Wt_\theta{}^{-1},$$
$$q_n=v_qt_\phi^{-1},\quad q_d=v_qC_w{}^{-1}. \tag{10}$$

The masses of the neutral gauge bosons are given by

$$M^2(Z_S)\sim\frac{g^2}{2}\left(m_l^2+l_l^2+q_l^2+\delta_{ld}+\delta_{nl}\right)\ ,$$
$$M^2(Z_H)\sim\frac{g^2}{2}\left(m_n^2+l_n^2+q_n^2+\delta_{nd}-\delta_{nl}\right)\ ,$$
$$M^2(Z_L)\sim\frac{g^2}{2}\left(l_d^2+q_d^2-\delta_{ld}-\delta_{nd}\right)\ , \tag{11}$$

where

$$\delta_{nd}\sim(q_nq_d-l_nl_d)\tan\theta_{nd}\ ,$$
$$\delta_{ld}\sim(l_ll_d-q_lq_d)\tan\theta_{ld}\ ,$$
$$\delta_{nl}\sim-(q_nq_l+l_nl_l)\tan\theta_{nl}\ .$$

III. RADIATIVE CORRECTIONS AND FORMULAS

The cross sections are usually calculated using the Born approximation for processes in which either a photon or a Z is exchanged and a fermion pair is emitted. The fermion f may be a charged lepton (e,μ,τ), a neutrino (ν_e,ν_μ,ν_τ), or one of five quark flavors (u,d,s,c or b). The energy dependence of Z production is described by a relativistic Breit-Wigner line shape and the cross section near the Z pole is enhanced by a factor of order of $\left(\frac{m_Z}{\Gamma_Z}\right)^2\sim10^3$. This is quite prominent compared to the nonresonant Bhabha scattering of the order of $\sim \frac{4\pi\alpha^2}{3s}$. However, the Born approximation is not adequate for the analysis of LEP experiments and it is essential to include the higher-order radiative corrections for the SM [5]. In general,the existence of a new heavy neutral vector boson Z_H leads to modifications of the coupling of the physical Z, to the fermions through the mixing angle ϕ. Similar modifications occur in the FUM through the mixing angle ϕ and θ due to the presence of Z_H and Z_S. In the extended models we have neglected the loop effects due to heavy neutral gauge bosons in comparison with their tree level effects under the assumption that the loop effects are dominated by the SM radiative corrections. The SM radiative corrections normally include (i) QED corrections from initial and final state photon radiation, (ii) QCD corrections from final state gluon radiation, (iii) weak corrections arising from the vertex and propagators, etc. The first correction is factored out from experimental data. The other corrections are small and calculable in the SM. However, they depend on the Higgs boson and top-quark masses and the value of the strong coupling constant α_s which are not yet very well determined experimentally. The dominant effects of these corrections can be summarized by replacing $\sin^2\theta_W$ by an effective mixing angle $\overline{\sin^2\theta_W}$,

$$\overline{\sin^2\theta_W} = \frac{1}{2} - \sqrt{\frac{1}{4} - \frac{\mu^2}{\rho_f M_Z^2(1-\Delta\alpha)}} \tag{12}$$

and also by replacing α by its renormalized value at the Z peak,

$$\alpha(M_Z^2) = \frac{\alpha}{1-\Delta\alpha} = 1.064\alpha, \tag{13}$$

by inserting the factor $\rho_f = \frac{1}{(1-\Delta\rho_f)}$ in the relationship between M_W and M_Z,

$$\frac{M_W^2}{M_Z^2} = \rho_f \overline{\cos^2\theta_W} \ ,$$

$$\frac{\pi\alpha(M_Z^2)}{\sqrt{2}G_F} = \rho_f M_Z^2 \overline{\sin^2\theta_W}\,\overline{\cos^2\theta_W} \ ,$$

$$\mu^2 = \frac{\pi\alpha(M_Z^2)}{\sqrt{2}G_F} = (37.280)^2 \tag{14}$$

with $\Delta\rho_f = \Delta\rho_T$ where

$$\Delta\rho_T = 0.0026 m_t^2 - 0.0015 \ln\left(\frac{m_H}{M_W}\right) . \tag{15}$$

Here ρ_f is the value of the ρ parameter after radiative corrections when there is no extra Z. After Z_1-Z_2 mixing $\overline{\sin^2\theta_W}$ has been further modified to

$$\overline{\overline{\sin^2\theta_W}} = \frac{1}{2} - \sqrt{\frac{1}{4} - \frac{\mu^2}{\rho M_Z^2(1-\Delta\alpha)}} \ , \tag{16}$$

where $\overline{\overline{\sin^2\theta_W}}$ is the effective $\sin^2\theta_W$ in the presence of mixing and the ρ parameter has been modified to

$$\rho = \rho_T \rho_M \ . \tag{17}$$

It may be noted that the parameter $\Delta\rho_M$ also gets a contribution ($\Delta\rho_{\rm SB}$) from the nonminimal Higgs structure, which is not taken into account separately in the present analysis. The number of color C also gets modified with the inclusion of second-order corrections as

$$C\left(1 + \frac{\alpha_s}{\pi} + \frac{1.4\alpha_s^2}{\pi^2}\right) \sim C(1+0.04) \ . \tag{18}$$

Thus the major radiative correction for $e^+e^- \to f\overline{f}$, except $b\overline{b}$ processes, can be estimated. The latter process requires an additional term that takes into account the relatively large t-b amplitude in the vertex correction and one has to make the substitution

$$\rho_b = \rho_f(1 - \tfrac{4}{3}\Delta\rho_T) \ ,$$
$$\overline{\overline{\sin^2\theta_b}} = \overline{\overline{\sin^2\theta_W}}(1 + \tfrac{2}{3}\Delta\rho_T) \ . \tag{19}$$

The final replacement is made for the tree level constant width pole structure $\left(s - M_Z{}^2 + iM_Z\Gamma_Z\right)^{-1}$ in the Z propagator with

$$\left(s - M_Z{}^2 + i\frac{s\Gamma_Z}{M_Z}\right)^{-1} . \tag{20}$$

The decay width of a Z boson into a fermion-antifermion ($f_i\overline{f}_i$) pair for the tree level diagram is given by

$$\Gamma(Z \to f_i\overline{f_i}) = \frac{CM_Z}{12\pi}(g_{A,i}^2 + g_{V,i}^2) \ , \tag{21}$$

where $g_{V,i}$ and $g_{A,i}$ are the vector and axial vector couplings of the neutral bosons to the fermions f_i. The $g_{V,i}$ and $g_{A,i}$ are given for the two models in Ref. [9]. For one generation of leptons and quarks the total decay width is obtained as

$$\Gamma(Z \to \text{all}) = \Gamma(Z \to e^+e^- + \nu_e\overline{\nu_e} + u\overline{u} + d\overline{d}) \ . \tag{22}$$

The width for three generations of leptons and quarks is obtained by multiplying each part of Eq. (22) by 3 except for the down quarks as the b quark contribution is calculated separately and added linearly.

The spin-averaged cross section for $e^+e^- \to f_i\overline{f_i}$ in units of the point cross-section $\sigma_{\rm pt} = \frac{4\pi\alpha^2}{3s}$ in the improved Born approximation is given by

$$R_i = \frac{\sigma\left(e^+e^- \to f_i\overline{f}_i\right)}{\sigma_{\rm pt}}$$
$$= C\left[\left(\frac{e_i}{e}\right)^2 + \sum\frac{(g_{V,e}{}^{j2} + g_{A,e}{}^{j2})(g_{V,i}{}^{j2} + g_{A,i}{}^{j2})}{e^4}\right.$$
$$\left.\times|\chi_j|^2 s^2 - \sum 2\left(\frac{e_i}{e}\right)\frac{g_{V,e}g_{V,i}}{e^2}\mathrm{Re}(\chi_j)s + X\right] \ , \tag{23}$$

where the Z_1-Z_2 interference term X is given by

$$X = 2\sum(g_{V,e}{}^j g_{V,e}{}^k + g_{A,e}{}^j g_{A,e}{}^k)(g_{V,i}{}^j g_{V,i}{}^k$$
$$+ g_{V,i}{}^j g_{V,i}{}^k)\mathrm{Re}(\chi_j\chi_k) \tag{24}$$

and

$$\chi_j = \frac{1}{(s - M_{Zj}{}^2 + i\frac{s\Gamma_{Zj}}{M_{Zj}})} \,. \tag{25}$$

e_i is the charge of the ith fermion and j is the index for different Z of our models. Here s is the center-of-mass energy squared. The expression for R_i in terms of the semiweak constant g, mixing angle ϕ, and θ (for the second model) can be obtained by incorporating g_A's and g_V's for different Z's of a particular model.

For the annihilation of a longitudinally polarized electron of helicity $\frac{1}{2}h$ and creation of a fermion of helicity $\frac{1}{2}h'$ the differential cross section is

$$\frac{d\sigma}{d\omega}(h,h')(e^+e^- \to f_i\overline{f_i}) = \frac{\alpha^2 C}{8s}\Bigg\{\Bigg[\left(\frac{e_i}{e}\right)^2 + (g_{V,e}^2 + g_{A,e}^2 + 2hg_{V,e}g_{A,e})\,\frac{g_{V,i}^2 + g_{A,i}^2 + 2h'g_{V,i}g_{A,i}}{e^4}|\chi|^2 s^2$$
$$-2\frac{e_i}{e}\frac{(g_{V,i} + hg_{A,i})(g_{V,e} + h'g_{A,e})}{e^2}\text{Re}\chi s\Bigg]\left[(1+\cos^2\theta_s) + 2hh'\cos\theta_s\right]\Bigg\} \,. \tag{26}$$

The symbol θ_s stands for the scattering angle between the incoming electron and outgoing fermion. The angular forward-backward (FB) asymmetry in $e^+e^- \to f_i\overline{f}_i$ is given by

$$A_{\text{FB}}^f(s,\theta_s) = \frac{d\sigma_f(\theta_s) - d\sigma_f(\pi - \theta_s)}{d\sigma_f(\theta_s) + d\sigma_f(\pi - \theta_s)}. \tag{27}$$

It is customary to define [8] $A_{\text{FB}}^f(s,\theta_s)$ at $\theta_s = 0$ and we have used this definition in the first part of the analysis. From Eqs. (25) and (26) we obtain the contributions of all the neutral Z bosons in a particular model to the angular FB asymmetry:

$$A_{\text{FB}}(s) = \Bigg[\sum\left(\frac{2g_{A,e}{}^j g_{A,i}{}^j}{e^2}\right)\left(\frac{2g_{V,e}{}^j g_{V,i}{}^j}{e^2}\right)|\chi_j|^2 s^2 - \sum\left(\frac{e_i}{e}\right)\left(\frac{2g_{A,e}{}^j g_{A,i}{}^j}{e^2}\right)$$
$$\times\text{Re}\chi_j s + X_1'\Bigg] \times \Bigg[\left(\frac{e_i}{e}\right)^2 + \sum\frac{\left(g_{V,e}{}^{j2} + g_{A,e}{}^{j2}\right)\left(g_{V,i}{}^{j2} + g_{A,i}{}^{j2}\right)}{e^4}|\chi_j|^2 s^2$$
$$-2\sum\left(\frac{e_i}{e}\right)\left(\frac{g_{V,e}{}^j g_{V,i}{}^j}{e^2}\right)\text{Re}\chi_j s + X_2'\Bigg]^{-1} \,. \tag{28}$$

The Z_1-Z_2 interference terms X_1' and X_2' are given by

$$X_1' = 2\sum\left(g_{A,e}{}^j g_{A,e}{}^k g_{A,i}{}^j g_{A,i}{}^k\right)\text{Re}(\chi_1\chi_2) \,,$$
$$X_2' = 2\sum(g_{V,e}{}^j g_{V,e}{}^k g_{V,i}{}^j g_{V,i}{}^k)\text{Re}(\chi_1\chi_2) \,, \tag{29}$$

where j and k are indices for different Z bosons of the model concerned. For the second part of the analysis we have used the integrated version of the forward-backward asymmetry in

$$A_{\text{FB}}^f(s) = \frac{\int_0^1 \frac{d\sigma_f}{d\cos\theta_s}d\cos\theta_s - \int_{-1}^0 \frac{d\sigma_f}{d\cos\theta_s}d\cos\theta_s}{\int_0^1 \frac{d\sigma_f}{d\cos\theta_s}d\cos\theta_s + \int_{-1}^0 \frac{d\sigma_f}{d\cos\theta_s}d\cos\theta_s}. \tag{30}$$

This parameter at the Z peak can be expressed as

$$A_{\text{FB}}^f(M_z^2) = 3\frac{g_{V,e}g_{A,e}g_{V,f}g_{A,f}}{(g_{V,e}^2 + g_{A,e}^2)(g_{V,f}^2 + g_{A,f}^2)}. \tag{31}$$

The τ-polarization asymmetry is defined by

$$A_{\text{pol}}^\tau = \frac{\sigma(e^+e^- \to \tau_L\overline{\tau}) - \sigma(e^+e^- \to \tau_R\overline{\tau})}{\sigma(e^+e^- \to \tau_L\overline{\tau}) + \sigma(e^+e^- \to \tau_R\overline{\tau})}. \tag{32}$$

This asymmetry parameter at the Z peak is given by

$$A_{\text{pol}}^\tau(M_z^2) = \frac{2g_{V,f}g_{A,f}}{g_{V,f}^2 + g_{A,f}^2}. \tag{33}$$

IV. RESULTS

In view of our previous results [9] regarding the impossibility of distinguishing the ununified models from the SM through the measurement of A, B, C_L, and the possibility of their discrimination only through the measurement of C_R, which, however, is not easily accessible to the experiment at present, we have adopted two methodologies to address the question of distinguishability of these models. First we have calculated $\sigma_{\text{total}}(e^+e^- \to f\overline{f})$ and $A_{\text{FB}}^f(s,\theta_s)(e^+e^- \to f\overline{f})$ near the Z resonance in the energy range 40 GeV$\leq \sqrt{s} \leq$ 160 GeV in the PUM and FUM and compared these values with those in the SM. The second part of our analysis is based on a two-parameter and three-parameter fit within the PUM to six precision LEP data: Γ_Z, σ_h^{peak}, $R = \frac{\Gamma_h}{\Gamma_l}$, $A_{\text{FB}}^l(M_Z^2)$, $A_{\text{FB}}^b(M_Z^2)$, and $A_{\text{pol}}^\tau(M_Z^2)$ at the Z pole ($M_Z = 91.187$ GeV). This part of our analysis is similar to that of Ref. [5].

In the first part of our analysis, we assume the mass hierarchy of the Z bosons as $M_{Z_L} < M_{Z_H} < M_{Z_S}$ so that M_{Z_L} corrosponds to the Z boson of the SM. M_{Z_H} ($\geq$ 500 GeV) in the PUM constrains ϕ to be $\sim 5°$ and M_{Z_H} and M_{Z_S} ($\geq$ 700 GeV) in the FUM results into $\theta = 5°$ and $\phi = 40°$. In the PUM the other arbitrary parameter is $x(= \frac{u^2}{v^2})$, the ratio of VEV's of the Higgs

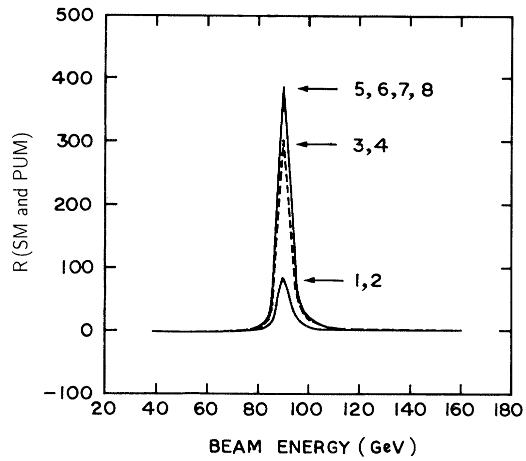

FIG. 1. The total cross section σ_i for $e^+e^- \to \overline{f_i}f_i$ for a partially ununified (1,3,5,7) as well as standard (2,4,6,8) model as a function of c.m. energy.

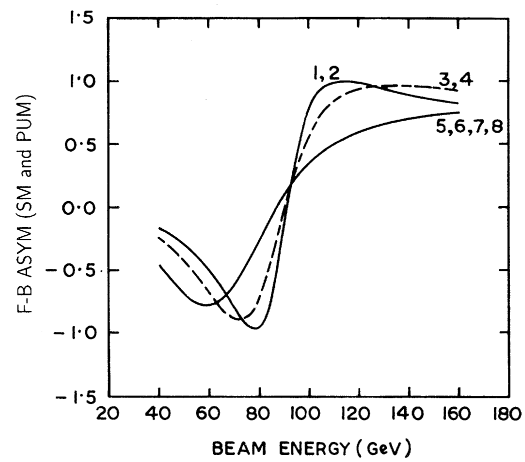

FIG. 3. The FB asymmetry vs c.m. energy for the partially ununified (1,3,5,7) and standard (2,4,6,8) model in the process $e^+e^- \to \overline{f_i}f_i$.

bosons in the model and similar parameters in the FUM are $x_1 = \frac{v_l}{v_q}$ and $x_2 = \frac{u}{\sigma}$. In the context of the PUM, we have calculated the total cross sections and angular FB asymmetry for the processes $e^+e^- \to f\overline{f}$ for a wide range of c.m. energy 40 GeV $\leq \sqrt{s} \leq$ 160 GeV with $\phi = 5°$ and x=1. Similar calculations have been performed in the FUM with $\phi = 40°$ and $\theta = 5°$. The Z_L-Z_H interference terms in Eq. (23b) and Eq. (28) are of the order of 10^{-8} for the above range of $\sqrt{s}$ and hence neglected. We have assumed the top and Higgs boson masses to be $m_t = m_H = 100$ GeV and thereby fixing

$$\overline{\sin^2\theta_{\rm W}} = 0.234, \quad \overline{\overline{\sin^2\theta_{\rm W}}} = 0.233 \tag{34}$$

implying constraint on $\Delta\rho_M$. Figure 1 shows the plot of the ratio $\frac{\sigma(e^+e^- \to f\overline{f})}{\sigma(e^+e^- \to e^+e^-)}$ in the PUM as a function of the c.m. energy in the range of 40 GeV $\leq \sqrt{s} \leq$ 160 GeV, where the final $f\overline{f}$ channel refers to l^+l^-, $u\overline{u}$, $d\overline{d}$, and $b\overline{b}$.

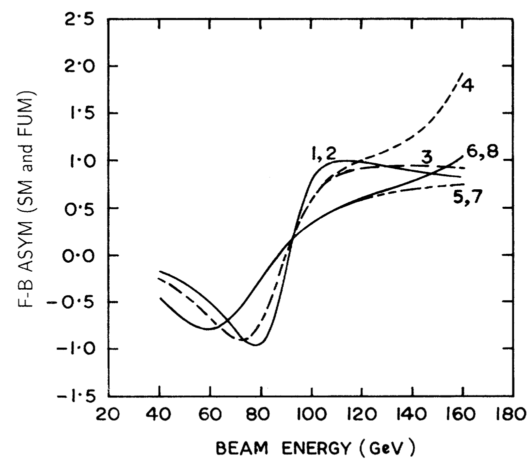

FIG. 4. The FB asymmetry vs c.m. energy for the fully ununified (1,3, 5,7) and standard (2,4,6,8) model in the process $e^+e^- \to \overline{f_i}f_i$.

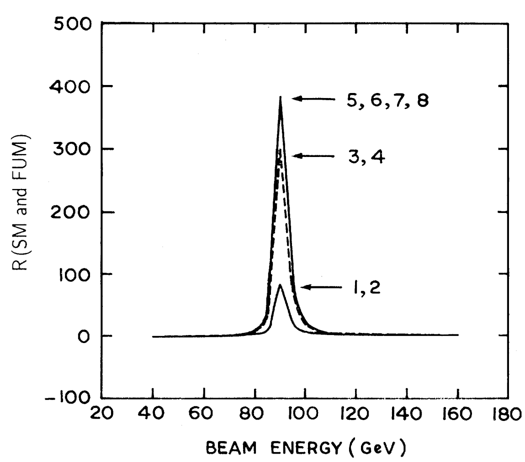

FIG. 2. The total cross section σ_i for $e^+e^- \to \overline{f_i}f_i$ for a fully ununified (1,3,5,7) as well as standard (2,4,6,8) model as a function of c.m. energy.

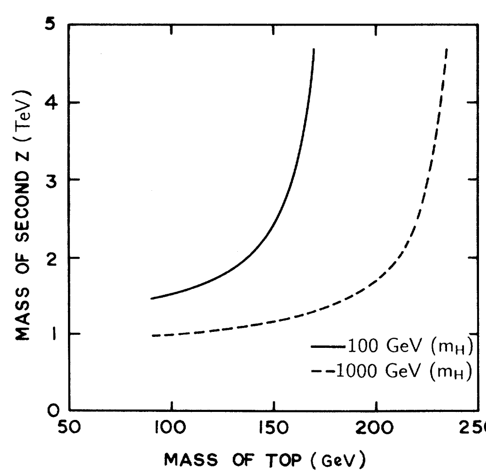

FIG. 5. Plot of the lower mass bound of the second Z vs top mass in PUM from the LEP data.

TABLE I. Combined fit of LEP data for PUM with $\Delta\rho_M$ and ϕ as two arbitrary free parameters.

m_t (GeV)	m_H (GeV)	$\Delta\rho_M$	ϕ(rad)	$\chi^2/N_{\rm DF}$
	100	0.0027± 0.0028	0.0301± 0.025	1.49/4
100	1000	0.0110± 0.0030	0.0208± 0.029	1.62/4
	100	-0.0003± 0.0028	0.0325± 0.025	1.51/4
135	1000	0.0083± 0.0031	0.0243± 0.029	1.63/4
	100	-0.0019± 0.0028	0.0339± 0.026	1.51/4
155	1000	0.0064± 0.0030	0.0264± 0.029	1.64/4
	100	-0.0035± 0.0030	0.0353± 0.024	1.52/4
170	1000	0.0048± 0.0035	0.0280± 0.029	1.65/4

The values of the ratio in the PUM for these channels (labeled as 1,3,5,7, respectively) are compared with the same in the SM (labeled as 2,4,6,8) for the corresponding channels. Similar comparison has been made in the FUM and is displayed in Fig. 2. Figure 3 shows the plots of $A^l_{\rm FB}(s,\theta_s)$, $A^u_{\rm FB}(s,\theta_s)$, $A^d_{\rm FB}(s,\theta_s)$, and $A^b_{\rm FB}(s,\theta_s)$ (labeled as 1, 3, 5, 7, respectively) at $\theta_s = 0$. Figure 4 shows the same plots in the FUM. These plots clearly demonstrate that the PUM and FUM cannot be discriminated from the SM through measurement of total cross sections and angular FB asymmetries in $e^+e^- \to l\bar{l}$, $u\bar{u}$, $d\bar{d}$, and $b\bar{b}$ processes.

In the second part of our analysis we have used six independent data $[\Gamma_Z, \sigma_h^{\rm peak}, R = \frac{\Gamma_h}{\Gamma_l}, A^l_{\rm FB}(M_Z^2), A^b_{\rm FB}(M_Z^2), A^\tau_{\rm pol}(M_Z^2)]$ for χ^2 analysis and made two-parameter and three-parameter fits using $\alpha_s = 0.12$, m_t in the range 100–170 GeV and m_H in the range 100–1000 GeV. The Z mass is fixed at the central value $M_Z = 91.187$ GeV. To obtain constraints on the fitted parameters we construct a χ^2 function

$$\chi^2 = \sum_{i,j} \frac{X_i^{\rm th} - X_i^{\rm expt}}{\sigma_i}[C_{ij}^{-1}]\frac{X_j^{\rm th} - X_j^{\rm expt}}{\sigma_i} , \qquad (35)$$

where $X_i^{\rm th}$ is the theoretical expression of ith observable in the PUM with the corresponding experimental results $X_i^{\rm expt} \pm \sigma_i$, σ_i is the standard deviation on $X_i^{\rm expt}$, and C represents the matrix of correlation.

The results of the two-parameter and three-parameter fits to the LEP data in the PUM are presented in Tables I and II, respectively. Using x=1, $m_t = m_H = 100$ GeV we have obtained from the two-parameter fit $\Delta\rho_M = 0.0027 \pm 0.0028$ and ϕ(rad) $= 0.0301\pm 0.025$. This indicates that $\Delta\rho_M$ and ϕ are consistent with zero implying the indistinguishability of the PUM from the SM. Interestingly, the central value of $\Delta\rho_M$ is seen decreasing with increasing m_t and ϕ is found to increase with increase in m_t. Keeping $m_t = 100$ GeV and increasing m_H from 100 to 1000 GeV, we obtain $\Delta\rho_M = 0.0110\pm 0.0030$ and $\phi = 0.0208\pm 0.0290$. The values of $\Delta\rho_M$ and ϕ remains essentially the same within errors in the three-parameter fit but the fitted value of x is $\sim 13.6 \pm 2.1$, which is surprisingly higher compared to unity leading to rather high value of the lower bound of the extra Z boson mass. This bound for $m_t = m_H = 100$ GeV turns out to be $M_{Z_H} \geq 1.46$ TeV. Figure 5 shows the variation of M_{Z_H} with the top mass m_t and Higgs boson mass m_H. With $m_H = 100$ GeV, M_{Z_H} increases with increase in m_t. Furthermore, M_{Z_H} decreases with increase in m_H. In particular, for $m_t = 100$ GeV and $m_H = 1000$ GeV, $M_{Z_H} \geq 988$ GeV. The influence of the radiative corrections is seen in the values of $\overline{\sin^2\theta_W}$ and $\overline{\overline{\sin^2\theta_W}}$ which turns out to be $\overline{\sin^2\theta_W} = 0.2323$ and $\overline{\overline{\sin^2\theta_W}} = 0.2311$ for $m_t = m_H = 100$ GeV. It may be noted that, for m_H= 100 GeV and m_t in the range between 100 and 170 GeV, the change in $\overline{\sin^2\theta_W}$ and $\overline{\overline{\sin^2\theta_w}}$ are about -0.0016 and -0.0003 approximately. However, for $m_t = 100$ GeV and m_H ranging from 100 GeV to 1000 GeV, the changes in $\overline{\sin^2\theta_W}$ and $\overline{\overline{\sin^2\theta_W}}$ are ~ 0.0028 and ~ 0.0001. Similar analysis in the framework of the FUM is expected not to yield any new interesting result other than the lower bound of the second extra Z boson mass which is of the order of several TeV.

TABLE II. Combined fit of LEP data for PUM with three arbitrary parameters $\Delta\rho_M$,ϕ (extra mixing angle) and x (ratio of VEV's).

m_t (GeV)	m_H (GeV)	$\Delta\rho_M$	ϕ (rad)	x	$\chi^2/N_{\rm DF}$
	100	0.0029± 0.0033	0.1113± 0.122	13.6± 2.1	1.50/3
100	1000	0.0112± 0.0030	0.0799± 0.154	13.7± 2.6	1.62/3
	100	0.0002± 0.0033	0.1215± 0.122	13.8± 2.2	1.51/3
135	1000	0.0085± 0.0033	0.0916± 0.154	13.8± 2.7	1.63/3
	100	-0.0017± 0.0033	0.1279± 0.122	13.8± 2.4	1.51/3
155	1000	0.0065± 0.0032	0.0995± 0.153	13.9 ± 2.8	1.64/3
	100	-0.0038± 0.0032	0.1305± 0.121	14.0± 2.3	1.52/3
170	1000	0.0050± 0.0035	0.1050± 0.151	14.4±2.8	1.65/4

V. CONCLUSION

We have shown that the total cross section and the forward-backward asymmetry for $e^+e^- \rightarrow f\bar{f}$ in the partially and fully ununified models are comparable to those in the standard model for c.m. energy from 40 GeV to 160 GeV. Furthermore, we have made two-and three-parameter fits to the six precision LEP data $\Gamma_Z, \sigma_h^{\rm peak}$, $R = \frac{\Gamma_h}{\Gamma_l}$, $A^l_{\rm FB}(M_Z^2)$, $A^b_{\rm FB}(M_Z^2)$, and $A^\tau_{\rm pol}(M_Z^2)$ with $\alpha_s = 0.12$. The results of the two-parameter fit in terms of the extra mixing angle ϕ and $\Delta\rho_M$ (the tree level deviation in the standard model ρ parameter from unity) are $\Delta\rho_M = 0.0027 \pm 0.0028$ and ϕ(rad) $= 0.0301 \pm 0.0250$ with $\chi^2 = 1.49$ for 4 degrees of freedom. The three-parameter fit including the parameter x, the ratio between the VEV's of the Higgs boson yields $\Delta\rho_M = 0.0028 \pm 0.0033$, ϕ(rad) $= 0.1113 \pm 0.1220$, and x=13.6± 2.1 with $\chi^2 = 1.50$ for 3 degrees of freedom. The dependence of $\Delta\rho_M$ and ϕ on the top and Higgs boson masses has also been studied. For a given top mass there is a trend of increase in $\Delta\rho_M$ and decrease in ϕ with increase in m_H and the trend is reversed with increase in top mass for a given Higgs boson mass. However, our analysis shows that $\Delta\rho_M$ and ϕ are consistent with zero within two standard deviations confirming again the indistinguishability of the ununified models from the standard model.

ACKNOWLEDGMENTS

Two of us (D.B. and K.B.) acknowledge financial assistance from DST and CSIR, Govt. of India, respectively.

[1] L. Ronaldi, in *Proceedings of the XXVIth International Conference on High Energy Physics,* Dallas, Texas, 1992, edited by J. Sanford, AIP Conf. Proc. No. 272 (AIP, New York, 1993).

[2] R.N. Mohapatra, *Unification and Supersymmetry* (Springer, New York, 1986); T.G. Rizzo *et al.*, Phys. Rep. **183**, 193 (1989).

[3] J.C. Pati and A. Salam, Phys. Rev. D **10**, 275 (1974); R.N. Mohapatra and J.C. Pati, *ibid.* **11**, 566 (1975); **11**, 2559 (1975); G. Senjanovic and R.N. Mohapatra, *ibid.* **12**, 152 (1975); G. Senjanovic, Nucl. Phys. **B153**, 334 (1979).

[4] J.L. Hewett and T.G. Rizzo, Phys. Rep. **183**, 193 (1989), and references cited therein; T.G. Rizzo, Phys. Rev. D **44**, 202 (1991).

[5] G. Altarelli, R. Casalbuoni, D. Dominici, F. Feruglio, and R. Gatto, Phys. Lett. B **245**, 669 (1990); Nucl. Phys. **B342**, 15 (1990); G. Altarelli, R. Casalbuoni, S. De Curtis, N. Di Bartolomeo, F. Feruglio, and R. Gatto, Phys. Lett. B **263**, 495 (1991); H. Burkhardt and J. Steinberger, Annu. Rev. Nucl. Part. Sci. **41**, 1 (1991); G. Bhattacharyya, A. Dutta, S.N. Ganguli, and A. Raychaudhuri, Mod. Phys. Lett. A **6**, 2557 (1991).

[6] H.M. Georgi, E.E. Jenkins, and E.H. Simmons, Phys. Rev. Lett. **62**, 2789 (1989); **63**, 1504(E) (1989).

[7] D. Choudhury, Mod. Phys. Lett. A **6**, 1185 (1991).

[8] V. Barger and T. Rizzo, Phys. Rev. D **41**, 946 (1990); T. Rizzo, Int. J. Mod. Phys. A **7**, 91 (1992); S. Rajpoot, Phys. Rev. D **41**, 995 (1990); L. Randall, Phys. Lett. B **234**, 508 (1990); K. Niyogi *et al.*, J. Phys. G **10**, 289 (1984).

[9] K. Bandyopadhyay, D. Bhowmick, A.K. Ray, and U. Sarkar, Phys. Rev. D **46**, 914 (1992).